

Influence of the Endothelial Surface Layer on Blood Flow in Microvessels: Computer Modeling and Simulation ^{*} ^{**}

Andrey Kovtanyuk¹[0000-0002-3286-110X],
Altynai Mukambaeva²[0000-0001-8353-6748],
Varvara Turova¹[0000-0002-6613-3311], Irina Sidorenko²[0000-0003-4158-9416], and
Renée Lampe¹[0000-0002-1016-0249]

¹ School of Medicine, Klinikum rechts der Isar, Orthopedic Department, Research Unit for Pediatric Neuroorthopedics and Cerebral Palsy of the Buhl-Strohmaier Foundation, Technical University of Munich, Munich, Germany

andrei.kovtaniuk@tum.de, turova@ma.tum.de, renee.lampe@tum.de

² Mathematical Faculty, Chair of Mathematical Modelling, Technical University of Munich, Garching, Germany

altynai.mukambaeva@tum.de, sidorenk@ma.tum.de

Abstract. The paper describes a mathematical model of blood flow in capillaries with accounting for the endothelial surface layer (ESL). The influence of ESL is modeled by a boundary layer with zero flow velocity. Numerical simulations for different levels of the discharge hematocrit are conducted using the finite element method. The reliability of the results obtained is verified using known experimental data.

Keywords: Capillary blood flow · Endothelial surface layer · Finite element method.

1 Introduction

Modeling blood circulation in human brain requires understanding the dynamics of blood flow both in the entire vascular network and in an individual vessel. Assuming the blood flow in a vessel as a moving laminar Newtonian fluid, we describe it by the Poiseuille's law [16]:

$$Q = \frac{\pi}{128} \frac{D^4}{L\mu} \Delta p. \quad (1)$$

Here, the flow Q (volume flow rate) through a cylindrical tube is a function of the pressure difference Δp , the tube diameter D , and the length L of the tube.

^{*} This work was supported by the Klaus Tschira Foundation, Buhl-Strohmaier Foundation, and Würth Foundation.

^{**} Copyright ©2020 for this paper by its authors. Use permitted under Creative Commons License Attribution 4.0 International (CC BY 4.0).

The dynamic viscosity μ is a material property of the liquid, which reflects the internal resistance to shearing motions. This law is a reasonable approximation for the flow in large blood vessels. As the diameter of the blood vessel decreases, the behavior of the blood flow increasingly deviates from the Poiseuille's law. For small vessels, e.g. for capillaries, the blood cannot be considered as continuous fluid with a fixed viscosity. Instead, it is regarded as plasma with suspended red blood cells (RBCs), also called erythrocytes. Other elements of blood, as for example, white blood cells and platelets have negligible effects on the blood flow due to their tiny volume fractions. Thus, the blood in a microvessel can be considered as a two-phase liquid consisting of plasma and erythrocytes [2, 3], wherein the RBCs phase is modeled by a high viscosity substance. Numerical realization of the two-phase model of blood flow in capillaries can be carried out using the finite element method (see, e.g., [3]).

The RBCs have a tendency to migrate away from the vessel walls to the centerline, which causes the formation of cell-free regions near the vessel walls. Since the velocity increases towards the vessel centerline, the velocities of RBCs are higher than the average blood velocity. This means that there is a difference between the tube hematocrit (the volume fraction of RBCs in the vessel at a given time instant) and the discharge hematocrit (the volume fraction of RBCs collected at the end of the tube at a given time period); the latter is higher than the tube hematocrit. This phenomenon is called Fåhræus effect [14]. The discharge hematocrit level has a significant impact on the parameters of blood flow in microvessels [14–16].

As noted above, Poiseuille's law does not apply to microvessels. However, to estimate the resistance to blood flow in microvessels, it is possible, on the base of (1), to define the apparent or effective viscosity of blood, that is, the viscosity of a Newtonian fluid that would give the same volume flow rate for a given tube geometry and pressure difference. According to (1), the apparent viscosity is determined as

$$\mu_{app} = \frac{\pi}{128} \frac{D^4}{L} \frac{\Delta p}{Q}. \quad (2)$$

By calculating the blood flow Q for a given pressure drop Δp using the finite element method, we can find the apparent viscosity by formula (2) and compare it with experimental data to estimate the adequacy of the mathematical model.

Note that the microcirculatory hemodynamic parameters (e.g., on the apparent viscosity and flow resistance) are significantly influenced by the endothelial surface layer (ESL). The effect of ESL on blood circulation, as well as its characteristics are discussed in [12–14, 16]. Following [13], the term “Endothelial surface layer” (ESL) is used for a boundary layer in which the plasma motion is significantly retarded. In particular, the ESL includes the glycocalyx layer. A. Copley studied the endothelium-plasma interface and developed a concept in which an immobile layer of plasma at the vessel wall is present [4, 5]. In the present paper, the influence of ESL on the apparent viscosity is investigated by means of the boundary layer with zero velocity.

Construction of a mathematical model of blood flow in microvessels accounting for the influence of ESL allows us to determine adequate vessels resistances in the brain capillary network. It is important to calculate the cerebral pressure distribution, for example, using the algorithm proposed in [2]. In particular, it can be applied to find most dangerous pressure gradients to estimate the risk of bleeding in the germinal matrix of preterm infants.

2 Experimental Observations of the Apparent Viscosity

The dependence of the relative apparent viscosity μ_{rel} (the ratio of apparent viscosity to plasma viscosity) on the discharge hematocrit and vessel diameter both *in vitro* and *in vivo* is provided by T. Secomb and A. Pries [15]. The *in vitro* data corresponding to blood flow in a glass tube are represented by the following equation:

$$\mu_{rel} = 1 + (\mu_{0.45} - 1) \frac{(1 - H_D)^C - 1}{(1 - 0.45)^C - 1}, \quad (3)$$

where

$$\mu_{0.45} = 220 \exp(-1.3D) + 3.2 - 2.44 \exp(-0.06D^{0.645}) \quad (4)$$

and

$$C = (0.8 + \exp(-0.075))(-1 + (1 + 10^{-11}D^{12})^{-1}) + (1 + 10^{-11}D^{12})^{-1}. \quad (5)$$

In these equations, D denotes the diameter of the vessel (glass tube) in μm , and H_D is the discharge hematocrit. The parameter $\mu_{0.45}$ is the viscosity for $H_D = 0.45$ which is a typical hematocrit for humans.

The plots of the relative viscosity obtained by the formula (3) (*in vitro* data) for the levels of discharge hematocrit of 0.1, 0.3, and 0.5 are shown in Fig. 1.

Similar measurements *in vivo* are difficult due to technicalities of measuring the pressure drop in capillaries. Therefore, it was assumed that the reduction of the viscosity with increasing diameter of living vessels was similar to that in glass tubes. However, the estimates of the apparent viscosity obtained by Lipowsky et al. [7, 8] for blood flow in microvessels were much higher than expected from the *in vitro* data. An alternative parametric description that is consistent with the observed behavior *in vivo* was found by Pries et al. [11]:

$$\mu_{rel} = \left(1 + (\mu_{0.45}^* - 1) \frac{(1 - H_D)^C - 1}{(1 - 0.45)^C - 1} \left(\frac{D}{D - 1.1} \right)^2 \right) \left(\frac{D}{D - 1.1} \right)^2, \quad (6)$$

where

$$\mu_{0.45}^* = 6 \exp(-0.085D) + 3.2 - 2.44 \exp(-0.06D^{0.645}) \quad (7)$$

and C remains the same as in equation (5).

The plots of the relative viscosity obtained by the formula (6) (*in vivo* data) for the levels of discharge hematocrit of 0.1, 0.3, and 0.5 are shown in Fig. 2.

The difference between the *in vivo* and *in vitro* data can be explained by the presence of the endothelial surface layer on the inner surface of blood vessels, which has a significant effect on the blood flow.

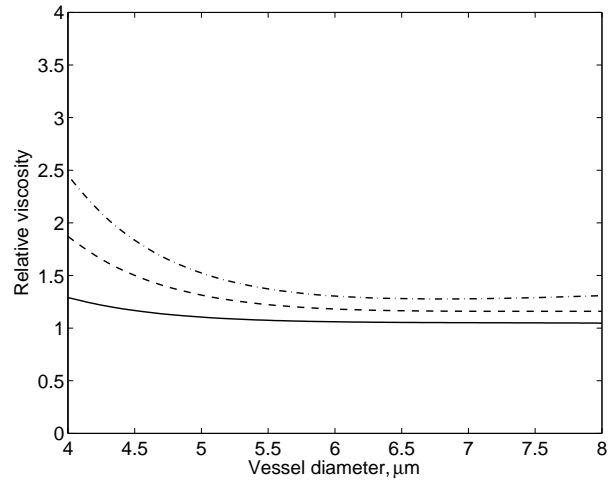


Fig. 1. Dependence *in vitro* of the relative viscosity (μ_{rel}) on the vessel diameter (D) for different values of the discharge hematocrit: $H_D = 0.1$ (solid line), $H_D = 0.3$ (dashed line), and $H_D = 0.5$ (dot-dashed line). The data represented by (3)-(5) correspond to the blood flow in glass tubes.

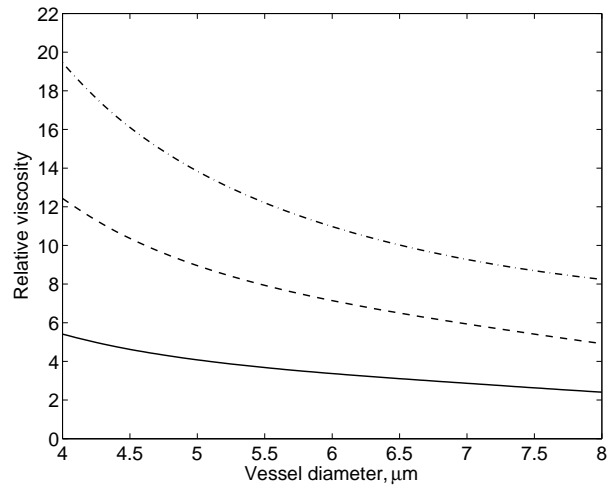


Fig. 2. Dependence *in vivo* of the relative viscosity (μ_{rel}) on the vessel diameter (D) for different values of the discharge hematocrit: $H_D = 0.1$ (solid line), $H_D = 0.3$ (dashed line), and $H_D = 0.5$ (dot-dashed line). The data represented by (6), (7) correspond to the blood flow in microvessels of animals.

3 Finite Element Modeling

As it was proposed in [2, 3], the RBCs and blood plasma are considered as one flow with two different viscosities (much larger viscosity for red blood cells): the viscosity of blood plasma is assumed to be $\mu_1 = 0.001 \text{ Pa} \cdot \text{s}$, whereas the viscosity of RBCs is set to be $\mu_2 = 0.1 \text{ Pa} \cdot \text{s}$ to make RBCs effectively rigid. Moreover, it is assumed that the flow is steady-state, without transition effects. Therefore, the model is described by the steady state Stokes equation with space variable viscosity.

Assume that the flow is axisymmetric, that is all variables depend only on the radial and longitudinal coordinates, r and z . Let u_r and u_z be the radial and longitudinal flow velocities, respectively, and p the pressure. Therefore, it is possible to reduce the problem to two dimensions (see Fig. 3). Here, the radius r_0 determines the boundary of the sequence of RBCs and hence $r_c - r_0$ is the thickness of the plasma gap between the RBCs and the vessel wall.

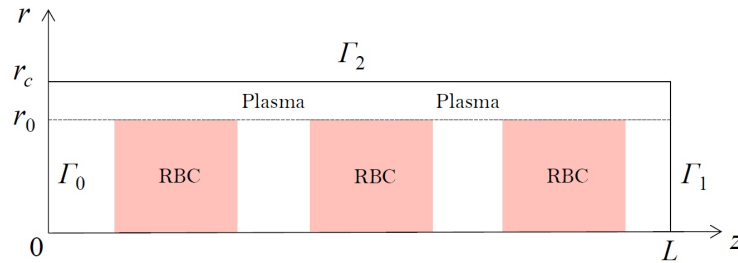


Fig. 3. Schematic drawing of the computational domain in cylindrical coordinates.

Denote $\Omega = (0, r_c) \times (0, L)$. The model is mathematically formulated in [17] in a weak form, which allows us to use spatially discontinuous viscosity functions. With $x_1 = r$, $x_2 = z$, $u_1 = u_r$, $u_2 = u_z$, $u = (u_1, u_2)^T$, $p(r, 0) = p_0$, $p(r, L) = 0$, the weak formulation reads in cylindrical coordinates as follows:

$$\int_{\Omega} x_1 \left(2\mu(x_1, x_2) \sum_{i,j=1}^2 D_{ij}(u) D_{ij}(v) + \frac{u_1 v_1}{x_1^2} \right) dx - \int_{\Omega} x_1 p \operatorname{div}(v) dx = \int_{\Gamma_0} x_1 p_0 v_2 dx, \quad (8)$$

$$\varepsilon \int_{\Omega} x_1 p q dx - \int_{\Omega} x_1 \operatorname{div}(u) q dx = 0, \quad \varepsilon = 10^{-6}, \quad u|_{\Gamma_2} = 0, \quad v|_{\Gamma_2} = 0, \quad (9)$$

where

$$D_{ij}(u) = \frac{1}{2} \left(\frac{\partial u_i}{\partial x_j} + \frac{\partial u_j}{\partial x_i} \right), \quad \operatorname{div}(u) = \frac{u_1}{x_1} + \frac{\partial u_1}{\partial x_1} + \frac{\partial u_2}{\partial x_2}.$$

Functions $v = (v_1, v_2)^T$, and q are the test ones. The viscosity distribution $\mu(x_1, x_2)$ is equal to $0.001 \text{ Pa} \cdot \text{s}$ in the plasma part and $0.1 \text{ Pa} \cdot \text{s}$ in the RBCs part.

Thus, the RBCs are modeled as fluid with the high viscosity to make them effectively rigid. The model (8), (9) is equivalent to the following one:

$$\int_{\Omega} x_1 \left(2\mu(x_1, x_2) \sum_{i,j=1}^2 D_{ij}(u) D_{ij}(v) + \frac{u_1 v_1}{x_1^2} + \nabla p v \right) dx = 0, \quad (10)$$

$$\varepsilon \int_{\Omega} x_1 (pq - \text{div}(u)q) dx = 0, \quad (11)$$

$$p|_{\Gamma_0} = p_0, \quad p|_{\Gamma_1} = 0, \quad u|_{\Gamma_2} = 0, \quad v|_{\Gamma_2} = 0, \quad (12)$$

where

$$\nabla p = \left(\frac{\partial p}{\partial x_1}, \frac{\partial p}{\partial x_2} \right).$$

To set the value of the pressure drop at a capillary with the length L , first, we estimate the pressure drop in the capillary network (pressure difference between inlets and outlets). For the estimation, the cerebral flow rate and total resistance of the capillary network are required. According to [18], the cerebral blood flow rate $Q = 600 \text{ ml/min}$ is a realistic value for an adult brain. Moreover, a cerebrovascular network model from [10] yields the total resistance R_T of the capillary system to be equal to $0.1 \text{ Pa} \cdot \text{s/mm}^3$, which gives the pressure drop to be equal to 1000 Pa (computed as $Q \cdot R_T$). Following [10], where the parallel topology for capillaries with the length of $600 \mu\text{m}$ and radius of $2.8 \mu\text{m}$ is utilized, we consider in further modeling that the pressure drop of 1000 Pa corresponds to the capillary length of $600 \mu\text{m}$. Therefore, for the capillary length equals to L , the pressure drop is $5L/3 \text{ Pa}$. In the numerical modeling, the capillary length is chosen in the range from 50 to $150 \mu\text{m}$ in accordance with the level of the hematocrit.

When conducting computer simulations, along with specifying the radius of the vessel, it is required to determine the radius r_0 of the core zone filled with RBCs and the linear dimensions of RBCs. To specify r_0 , we use the following approximation [2]:

$$r_0 = 0.3\mu\text{m} + 0.8r_c. \quad (13)$$

The length of an erythrocyte is determined on the base of its mean volume equals to $88 \mu\text{m}^3$ [9] and the value of r_0 .

Comparison of the results of the finite element modeling (conducted by using FreeFEM++ package [6]) with *in vitro* data shows a significant difference (see Fig. 4). This is because the velocity no-slip condition, $u|_{\Gamma_2} = 0$, is not suitable for modeling the blood flow in glass tubes. More adequate is using the velocity slip condition: $u_1|_{\Gamma_2} = 0$ and $\alpha \partial u_2 / \partial x_1 + u_2|_{\Gamma_2} = 0$. By appropriate choosing the parameter α in numerical modeling, we can provide a closer approximation of the *in vitro* data.

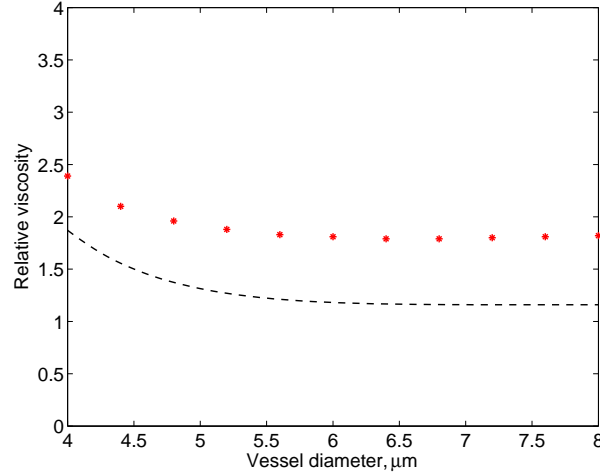


Fig. 4. *In vitro* data of the relative viscosity (μ_{rel}) calculated with (3)-(5) for $H_D = 0.3$ (dashed line), and the corresponding results of the finite element modeling (red asterisks).

To take into account the influence of ESL in modeling the blood flow in microvessels, we assume zero flow velocity in some neighborhood of the vessel wall, that is $u = 0$ for $r^* < r \leq r_c$ ($r^* > r_0$). The presence of the sublayer of ESL with zero flow velocity is mentioned in particular in [14], where the longitudinal velocity profile measured in a rat venule is presented. Note that a similar effect regarding zero velocity in a neighborhood of the surface somewhat akin to ESL is also observed [1] in modeling of elasto-optical biosensors.

To fit the results of finite elements modeling to experimental data described by (6) and (7), we use the following representation of the boundary of the layer with zero flow velocity:

$$r^* = 0.366\mu\text{m} + 0.725r_c + 0.024r_c^2. \quad (14)$$

The formula (14) is obtained by the minimization of the mean square error between the results of the finite element modeling and *in vivo* data given by (6). Note that the representation (14) was obtained under the assumption of the consistency of the approximation (13). Refining the formula (13) will result in a corresponding adjustment of the formula (14).

The computed values of the relative viscosity and *in vivo* data calculated with (6) and (7) are shown in Fig. 5.

It is worth to note that taking into account the influence of ESL through the layer with zero flow velocity is characterized by a significant increase of the relative viscosity and, respectively, by a proportional increase of the microvessel resistance. As a consequence, it leads to a proportional decrease in the longitudinal velocity. The results of a numerical experiment for the vessel diameter of $6 \mu\text{m}$ and $H_D = 0.3$ are shown in Fig. 6.

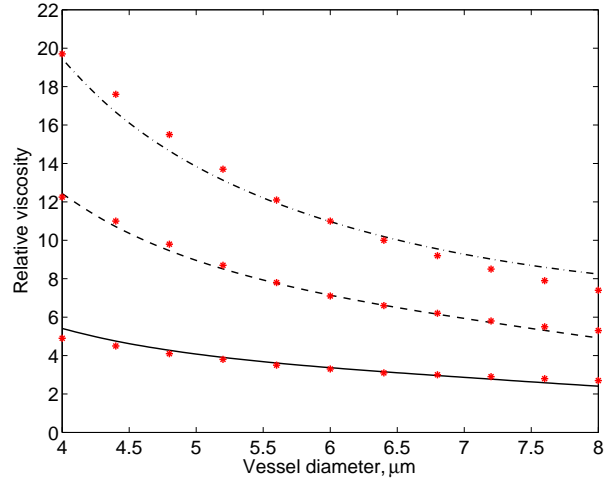


Fig. 5. *In vivo* data of the relative viscosity (μ_{rel}) calculated with (6) and (7) for different values of the discharge hematocrit: $H_D = 0.1$ (solid plot), $H_D = 0.3$ (dashed plot), and $H_D = 0.5$ (dots-dashed plot); and the corresponding results of the finite element modeling (red asterisk) using the approximations (13) and (14).

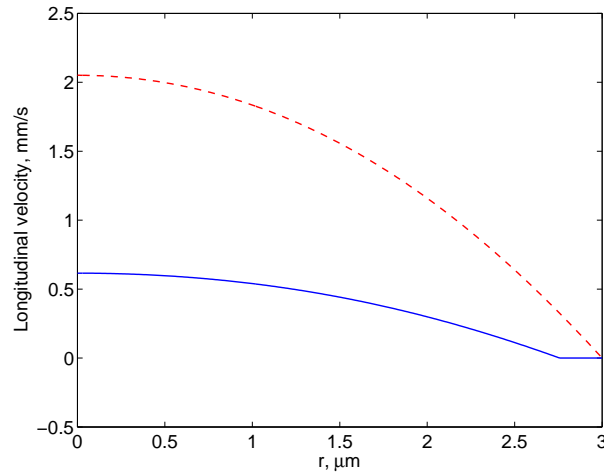


Fig. 6. Velocity profile (longitudinal velocity, u_2) for the vessel diameter of $6 \mu\text{m}$ and $H_D = 0.3$: with accounting for zero flow velocity layer (blue solid line) and without it (red dashed line).

In the example considered, accounting for the ESL leads to the 3.9-fold increase of the viscosity and, respectively, to the 3.9-fold decrease of the blood flow.

4 Conclusion

The mathematical model of blood flow in capillaries containing the endothelial surface layer was proposed. The ESL influence is described by the presence of the boundary layer with zero flow velocity. The reliability of the results obtained has been verified for different values of the discharge hematocrit and vessel diameter using experimental data from the literature.

Further efforts of the authors will be aimed at applying this approach to calculate the characteristics of the cerebral capillary network with the subsequent calculation of the blood flow and pressure drop distributions in the germinal matrix of preterm infants.

References

1. Botkin, N.D., Hoffmann, K.-H., Marx, D., Starovoitov, V.N., Turova, V.L.: Modeling in the development of an elasto-optical biosensor based on nanostructures. *Int. J. Biomath. Biostat.* **2**(2), 191–202 (2013)
2. Botkin, N.D., Kovtanyuk, A.E., Turova, V.L., Sidorenko, I.N., Lampe, R.: Direct modeling of blood flow through the vascular network of the germinal matrix. *Comp. Biol. Med.* **92**, 147–155 (2018)
3. Botkin, N.D., Kovtanyuk, A.E., Turova, V.L., Sidorenko, I.N., Lampe, R.: Accounting for tube hematocrit in modeling of blood flow in cerebral capillary networks. *Comp. Math. Meth. Med.* **2019**, 4235937 (2019)
4. Copley, A.L.: Hemorheological aspects of the endothelium-plasma interface. *Microvasc. Res.* **8**, 192–212 (1974)
5. Copley, A.L.: The endoendothelial fibrin lining, fibrinogen gel clotting, and the endothelium-blood interface. *Ann. N. Y. Acad. Sci.* **416**, 377–396 (1983)
6. Hecht, F.: New development in FreeFem++. *J. Numer. Math.* **20**(3-4), 251–265 (2012).
7. Lipowsky, H.H., Kovalcheck, S., Zweifach, B.W.: The distribution of blood rheological parameters in the microvasculature of cat mesentery. *Circ. Res.* **43**(5), 738–749 (1978)
8. Lipowsky, H.H., Usami, S., Chien, S.: In vivo measurements of apparent viscosity and microvessel hematocrit in the mesentery of the cat. *Microvasc. Res.* **19**(3), 297–319 (1980)
9. McLaren, C.E., Brittenham, G.M., Hasselblad, V.: Statistical and graphical evaluation of erythrocyte volume distributions. *Am. J. Physiol.* **252**, H857–H866 (1987).
10. Piechnik, S.K., Chiarelli, P.A., Jezzard, P.: Modelling vascular reactivity to investigate the basis of the relationship between cerebral blood volume and flow under CO₂ manipulation. *NeuroImage* **39**, 107–118 (2008)
11. Pries, A.R., Secomb, T.W., Gessner, T., Sperandio, M., Gross, J.F., Gaetgens, P.: Resistance to blood flow in microvessels in vivo. *Circ. Res.* **75**, 904–915 (1994).

12. Pries, A.R., Secomb, T.W., Jacobs, H., Sperandio, M., Osterloh, K., Gaehtgens, P.: Microvascular blood flow resistance: role of endothelial surface layer. *Am. J. Physiol.* **273**, H2272–H2279 (1997)
13. Pries, A.R., Secomb, T.W., Gaehtgens, P.: The endothelial surface layer. *Pflug. Arch. – Eur. J. Physiol.* **440**, 653–666 (2000)
14. Pries, A.R., Secomb, T.W.: Blood flow in microvascular networks. In: *Microcirculation*, pp. 3–36. Elsevier, Academic Press, Amsterdam (2008)
15. Secomb, T.W., Pries, A.R.: Blood viscosity in microvessels: experiment and theory. *Comptes Rendus Physique.* **14**(6), 470–478 (2013)
16. Secomb, T.W.: Blood flow in the microcirculation. *Annu. Rev. Fluid Mech.* **49**, 443–461 (2017)
17. Tabata, M.: Finite Element analysis of axisymmetric flow problems and its application. *Z. Angew. Math. Mech.* **76**, 171–174 (1996)
18. Walters, F.J.M.: Intracranial pressure and cerebral blood flow. *Update in Anaesthesia.* **8**, 18–23 (1998)